Model development for current–voltage and transconductance characteristics of normally-off AlN/GaN MOSHEMT

© R. Swain, K. Jena, T.R. Lenka

Microelectronics & VLSI Group, Department of Electronics & Communication Engineering,
National Institute of Technology Silchar,
Assam, 788010 India

E-mail: trlenka@gmail.com

(Получена 12 марта 2015 г. Принята к печати 8 июля 2015 г.)

In this paper, an AlN/GaN-based MOSHEMT is proposed, in accordance to this, a charge control model has been developed analytically and simulated with MATLAB to predict the characteristics of threshold voltage, drain currents and transconductance. The physics based models for 2DEG density, threshold voltage and quantum capacitance in the channel has been put forward. By using these developed models, the drain current for both linear and saturation models is derived. The predicted threshold voltage with the variation of barrier thickness has been plotted. A positive threshold voltage can be obtained by decreasing the barrier thickness which builds up the foundation for enhancement mode MOSHEMT devices. The predicted I_d–V_{gs}, I_d–V_{ds} and transconductance characteristics show an excellent agreement with the experimental results and hence validate the model.

1. Introduction

AlN/GaN High Electron Mobility Transistors (HEMTs) have evolved as the most promising microwave power devices having high power density during high frequency operations. This is possible as this device has unique properties such as wide band gap (6.2 eV of AlN to 3.4 eV of GaN), large breakdown electric field strengths (~ 3 MV/cm), high 2DEG density ($2 \cdot 10^{13}$ cm^{-2}), low relative dielectric constant (10.8 for AlN, 9.5 for GaN), high saturation electron drift velocity ($> 2 \cdot 10^7$ cm/s), high mobility (~ 1000 cm^2/V $\cdot$ s) and low sheet resistance ($< 150\,\Omega/\square$) [1]. The 2DEG concentration in the conventional AlGaN/GaN structure plays a vital role [2,3] and it has a strong dependence on the Al content in the AlGaN layer [4]. The highest 2DEG sheet charge density can be achieved with very thin barrier layer having 100% Al content. Literature reveals that for the 2DEG sheet density of $1.1 \cdot 10^{13}$ cm^{-2} only 5 nm thickness of AlN barrier layer is sufficient [5]. So AlN/GaN is an ideal combination for the realization of normally-off (E-mode) devices since due to a thin barrier it is easy to deplete the channel.

The MOSHEMT device incorporates an extra thin dielectric layer such as Al_2O_3 [6] under the gate to minimize the gate leakage current. Literature on E-mode AlN/GaN MOSHEMT device with regrown source and drain contact spacing value $L_{sd} = 0.7\,\mu$m reveals transconductance (g_m) of 509 mS/mm, maximum drain current I_d of 860 mA/mm, gate leakage current less than 1 mA/mm, ohmic contact resistance $0.153\,\Omega \cdot$ mm, on-resistance $1.63\,\Omega \cdot$ mm and I_{on}/I_{off} ratio up to 10^6 [7]. With self-aligned gate-last process cut-off frequency $f_T = 40$ GHz is obtained with a channel length (L_g) of 210 nm [8]. The compact charge based model for current–voltage and capacitance–voltage characteristics in AlGaN/GaN HEMT is presented with considering all the non-ideality factors in Refs [9,10]. The model for 2DEG density and threshold voltage considering interface DOS for MOSHEMT had been demonstrated in our recent work [11]. But there is a lack of model for MOSHEMT devices elucidating the current–voltage and transconductance behavior by considering quantum capacitance formed at 2DEG, and this forms the motivation behind the present work.

The organization of this paper is as follows. The model development is presented in Section 2 which includes the model for 2DEG density, threshold voltage, and drain currents (I_d–V_{gs} and I_d–V_{ds}). The MATLAB based simulation results of the developed model along with the experimental results from the literature for I_d–V_{gs}, I_d–V_{ds} and transconductance are plotted in Section 4. Finally the conclusion has been drawn in Section 4.

2. Model development

Fig. 1 shows a schematic diagram of the AlN/GaN heterostructure used in this study. It consists of a metal gate (Ni) followed by Al_2O_3, AlN barrier layer, an unintentionally doped GaN channel, a GaN semi-insulating buffer layer and substrate layer.

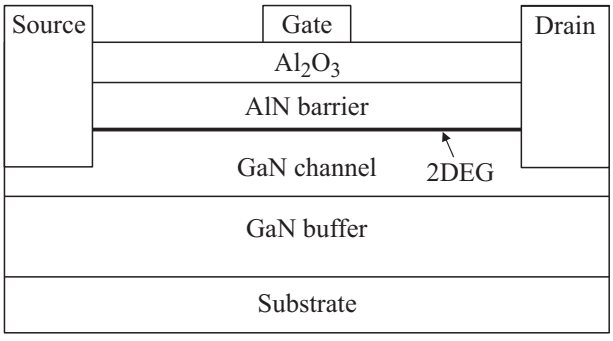

Figure 1. Proposed MOSHEMT structure.

For a HEMT the sheet charge concentration is given by [12]

$$n_s = \sigma_{\text{pol}} - \frac{\varepsilon_{\text{AlN}}}{q d_{\text{AlN}}}[\phi_s + E_{\text{F}}(n_s) - \Delta E_c], \tag{1}$$

where σ_{pol} is the induced charge concentration due to polarization, ε_{AlN} is the permittivity for AlN, q is the charge of electron, d_{AlN} is the barrier thickness; $E_{\text{F}}(n_s)$ is the Fermi potential in GaN layer, ϕ_s is the surface potential, and ΔE_c is the discontinuity of the conduction band at the AlN/GaN interface. The surface potential ϕ_s can be represented as $\phi_s = \phi_{s0} - V_{gs}$, ϕ_{s0} is the surface potential at zero gate potential and V_{gs} is the applied gate voltage.

2.1. Dependence of n_s on barrier thickness

Fig. 2 shows the energy band diagram of AlN/GaN MOSHEMT structure.

At absolute zero temperature ($T = 0$) all the levels above Fermi energy level are empty while those below it are filled with electrons. This results in the ionized state of the empty donor traps above Fermi level while the acceptor traps are neutral. An extra positive interface charge [13] contributed by these states in AlN/GaN MOSHEMTs at any temperature is given by

$$Q_{it} = D_{it} q \int_{E_{\text{F}_0}}^{E_{NL}} [1 - f_{\text{F}}(E)] dE. \tag{2}$$

Here D_{it} is the interface density of states (DOS), Q_{it} is the interface charge. It is to be noted that E_{NL} is the charge neutral level and E_{F_0} is the Fermi potential level at zero gate bias. $f_{\text{F}}(E)$ is the Fermi–Dirac probability of a donor interface state between E_{NL} and E_{F_0} being occupied and it is represented as

$$f_{\text{F}}(E) = \left\{ \frac{1}{1 + \exp[a(E - E_{\text{F}_0})/kT]} \right\}. \tag{3}$$

If we assume that $(E_{NL} - E_{\text{F}_0}) \gg kT/q$, the integration in Eq. (2) after putting limits reduces to the expression for oxide interface charge concentration similar to [14] as per Eq. (4),

$$Q_{it} = D_{it} q (E_{NL} - E_{\text{F}_0}). \tag{4}$$

The assumption is quite plausible because the occupancy probability of an energy level tends to zero after an energy just $3kT$ above E_{F_0}.

This depletion charge along with the oxide-barrier interface charge results in a potential drop V_{bi} and neglecting barrier capacitance it can be given by

$$V_{\text{ox}} = \frac{Q_D + Q_{it}}{C_{\text{oxide}}}, \tag{5}$$

where Q_D is the depletion charge in AlN and C_{oxide} is the oxide capacitance. The depletion charge can be formulated as

$$Q_D = q N_D d_{\text{AlN}}, \tag{6}$$

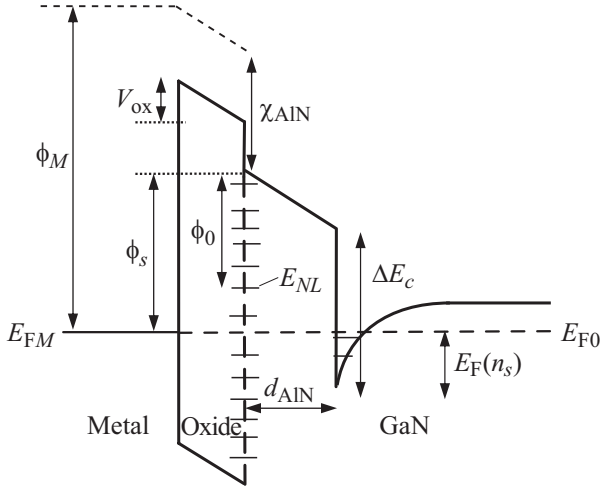

Figure 2. Conduction band profile for a metal/oxide/AlN/GaN interface.

where N_D is the unintentional doping concentration in AlN. Making use of Eqs (4)–(6) we get

$$V_{\text{ox}} = \frac{q N_D d_{\text{AlN}} + D_{it} q (E_{NL} - E_{\text{F}_0})}{C_{\text{oxide}}}. \tag{7}$$

Clearly from Fig. 2 we see that the surface potential $\phi_s = \phi_M - \chi_{\text{AlN}} - V_{\text{ox}}$ and $E_{NL} - E_{\text{F}_0} = \phi_s - \phi_0$, ϕ_M is the metal work function, χ_{AlN} is the electron affinity of AlN, V_{ox} is the residual oxide interface potential and ϕ_0 is the potential difference between the neutral level and the conduction band edge. Introducing these relations in Eq. (7) we get a relation between the surface potential and barrier thickness as follows

$$\phi_{s0} = \gamma(\phi_M - \chi_{\text{AlN}}) + (1 - \gamma)\phi_0 - \frac{\gamma q N_D d_{\text{AlN}}}{C_{\text{oxide}}}, \tag{8}$$

where $\gamma = 1/(1 + D_{it} q / C_{\text{oxide}})$, ϕ_{s0} represents surface potential when voltage applied at gate terminal is zero.

The dependence of the surface potential and hence 2DEG sheet charge density on the thickness can be seen from Eq. (1) and Eq. (8). Making use of these equations we will get the 2DEG sheet charge density as

$$n_s = \sigma_{\text{pol}} - \frac{\varepsilon_{\text{AlN}}}{q d_{\text{AlN}}} \times \left[\gamma(\phi_M - \chi_{\text{AlN}}) + (1 - \gamma)\phi_0 - \frac{\gamma q N_D d_{\text{AlN}}}{C_{\text{oxide}}} + E_{\text{F}}(n_s) - \Delta E_c \right]. \tag{9}$$

Now the only unknown in Eq. (9) is E_{F} which is a function of n_s itself and can be obtained as follows. The self-consistent solution of the Schrodinger and Poisson equations give rise to the following relation where two sub-band energy levels (E_0 and E_1) are considered [15]:

$$n_s = \frac{DkT}{q} \sum_{i=0,1} \ln\left\{ 1 + \exp\left[\frac{q(E_{\text{F}} - E_i)}{kT} \right] \right\}, \tag{10}$$

where $D = 4\pi m^*/h^2$ is the conduction band density of states of a 2D system, m^* is the electron effective mass

List of Model parameters

Parameter	Value	Unit
$\varepsilon_{\mathrm{AlN}}$	$10.78\varepsilon_0$	F/m^2
$\varepsilon_{\mathrm{oxide}}$	$9\varepsilon_0$	F/m^2
k_1	-0.0802	V
k_2	$1.039 \cdot 10^{-9}$	V · m
k_3	$1.0454 \cdot 10^{-18}$	V · m^2
ΔE_c	0.343	eV
σ_{pol}	$3.38 \cdot 10^{17}$	m^{-2}
t_{oxide}	6	nm
d_{AlN}	6	nm
ϕ_M	5.1	eV
χ_{AlN}	1.9	eV
ϕ_0	3.4	eV
N_D	$1.5 \cdot 10^{16}$	m^{-3}
D_{it}	$1.2 \cdot 10^{12}$	m^{-3}
Z/L_{sd}	200	
μ_n	0.09	m^2/V · s

in GaN, h is the Planck's constant, k is the Boltzmann's constant, T is the ambient temperature, $E_0 = c_0 n_s^{2/3}$ (in eV), and $E_1 = c_1 n_s^{2/3}$ (in eV) are the allowed energy levels in the well. Here c_0 and c_1 are determined by Robin boundary conditions [16,17]. The above equation shows the linear relationship between n_s and E_{F}. As the occupancy of sub-band energy levels inside the quantum well increases with increase in temperature [18], accordingly the inclusion of higher order energy sub-bands in Eq. (10) for calculation of 2DEG density is essential. However, this 2DEG dependent Fermi potential can be expressed by a more appropriate 2nd order expression by considering temperature effects as per Ref. [16], which gives a good fitting to the numerical solution of Eq. (9) as follows,

$$E_{\mathrm{F}} = k_1 + k_2 n_s^{1/2} + k_3 n_s, \tag{11}$$

where k_1, k_2 and k_3 are temperature dependent parameters and gave been calculated in Ref. [16]. Though finally the model results are compared to experimental results obtained at room temperature, so the values of k_1, k_2 and k_3 at 300 K are referred from Ref. [16] during model calculations and mentioned in Table. It is noteworthy that for higher temperatures these values are to be considered accordingly. Making use of Eq. (9) and Eq. (11) for solving n_s, we get

$$n_s = [-A + \sqrt{A^2 - (B + C\phi_s - F)}]^2, \tag{12}$$

where

$$A = \frac{\varepsilon_{\mathrm{AlN}} k_2}{2(\varepsilon_{\mathrm{AlN}} k_3 + q d_{\mathrm{AlN}})}, \tag{13}$$

$$B = \frac{\varepsilon_{\mathrm{AlN}}(k_1 - \Delta E_c)}{(\varepsilon_{\mathrm{AlN}} k_3 + q d_{\mathrm{AlN}})}, \tag{14}$$

$$C = \frac{\varepsilon_{\mathrm{AlN}}}{(\varepsilon_{\mathrm{AlN}} k_3 + q d_{\mathrm{AlN}})}, \tag{15}$$

$$F = \frac{d_{\mathrm{AlN}} q \sigma_{\mathrm{pol}}}{(\varepsilon_{\mathrm{AlN}} k_3 + q d_{\mathrm{AlN}})}. \tag{16}$$

2.2. Quantum capacitance model

The total capacitance across the MOSHEMT junction is given by [19] as follows,

$$C_{\mathrm{eq}} = \left[\frac{1}{C_{\mathrm{oxide}}} + \frac{1}{C_{it} + (1/C_b + 1/C_q)}\right]^{-1}. \tag{17}$$

Here C_{it} is the capacitance due to interface traps, C_b is the capacitance due to barrier layer charges and C_q is the quantum capacitance formed in 2DEG.

If we neglect the interface traps and assume that C_b is much greater than C_q, the total capacitance becomes

$$C_{\mathrm{eq}} = \frac{C_{\mathrm{oxide}} C_q}{C_{\mathrm{oxide}} + C_q}, \tag{18}$$

where C_{oxide} is the capacitance due to oxide layer and can be represented as

$$C_{\mathrm{oxide}} = \frac{\varepsilon_{\mathrm{oxide}}}{t_{\mathrm{oxide}}}, \tag{19}$$

$\varepsilon_{\mathrm{oxide}}$ is the oxide dielectric constant and t_{oxide} is the oxide layer thickness. The quantum capacitance is given by

$$C_q = \frac{\partial(q n_s)}{\partial \phi_s}. \tag{20}$$

Quantum capacitance originates at the 2DEG region due to penetration of Fermi level into conduction band. It can be obtained by differentiating the sheet charge density with respect to surface potential. Calculating the above differentiation we will find

$$C_q = q \frac{C[-A + \sqrt{A^2 - (B + C\phi_s - F)}]}{\sqrt{A^2 - (B + C\phi_s - F)}}. \tag{21}$$

2.3. Threshold voltage model

In order to make this MOSHEMT device completely off the 2DEG is to be pinched-off. As can be seen in Fig. 3 under this condition the difference in the energy of Fermi

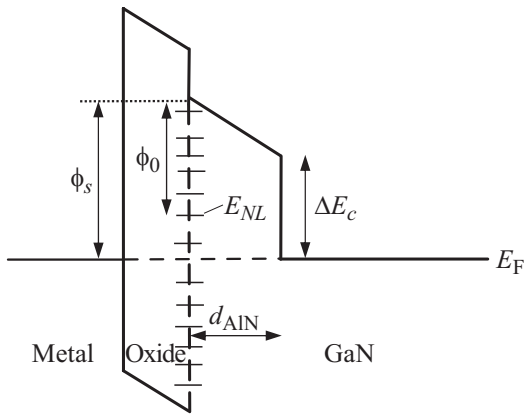

Figure 3. Conduction band at pinch-off.

level and the minimum energy of electron in 2DEG reduces to zero. So n_s and E_F becomes zero. Putting these two conditions and replacing ϕ_s with $\phi_s = \phi_{s0} - V_{th}$ in Eq. (9) where ϕ_{s0} is given by Eq. (8) and solving for V_{th} we get the expression for threshold voltage as shown in Eq. (22):

$$V_{th} = \gamma(\phi_M - \chi_{AlN}) + (1-\gamma)\phi_0 - \frac{\gamma q N_D d_{AlN}}{C_{oxide}} - \Delta E_c - \frac{\sigma_{pol}\sigma - d_{AlN}}{\varepsilon_{AlN}}. \quad (22)$$

This expression can be used in conventional HEMT current equation to find the linear and saturation mode drain current as follows [20]

$$I_{d,lin} = \frac{\mu_n c_{eq}}{2}\left(\frac{Z}{L_{sd}}\right)[2(V_{gs} - V_{th})V_{ds} - V_{ds}^2], \quad (23)$$

where μ_n is electron mobility at GaN surface, L_{sd} is length between source and drain, V_{gs} is the voltage applied between gate and source, V_{ds} is the voltage applied between drain and source. C_{eq} and V_{th} are given by Eqs (18) and (22), respectively.

Similarly, the saturation mode current equation is given by

$$I_{d,sat} = \frac{\mu_n c_{eq}}{2}\left(\frac{Z}{L_{sd}}\right)(V_{gs} - V_{th})^2. \quad (24)$$

The transconductance can be found by differentiating the drain current equation with respect to gate voltage as follows,

$$g_m = \frac{\partial I_{d,lin}}{V_{gs}}, \text{ when } V_{ds} \le V_{gs} - V_{th},$$

$$g_m = \frac{\mu_n c_{eq}}{2}\left(\frac{Z}{L_{sd}}\right)V_{ds}, \quad (25)$$

$$g_m = \frac{\partial I_{d,sat}}{V_{gs}}, \text{ when } V_{ds} > V_{gs} - V_{th},$$

$$g_m = \mu_n c_{eq}\left(\frac{Z}{L_{sd}}\right)(V_{gs} - V_{th}). \quad (26)$$

3. Simulation results and discussion

First of all Eq. (22) is plotted in MATLAB to see the variation of threshold voltage with respect to barrier thickness alone as shown in Fig. 4. The figure demonstrates that the threshold voltage varies inversely with barrier thickness at constant oxide thickness and can be pushed towards positive value by taking an extremely thin barrier. Further a positive threshold voltage is the basic requirement for an enhancement mode MOSHEMT and decreasing barrier thickness is a method to achieve this.

Then the drain current in Eqs (23) and (24) is plotted with respect to V_{ds} and V_{gs} in MATLAB to obtain $I_d - V_{ds}$ and $I_d - V_{gs}$ characteristics, respectively. Basic fitting method such as shape preserving interpolant is used to

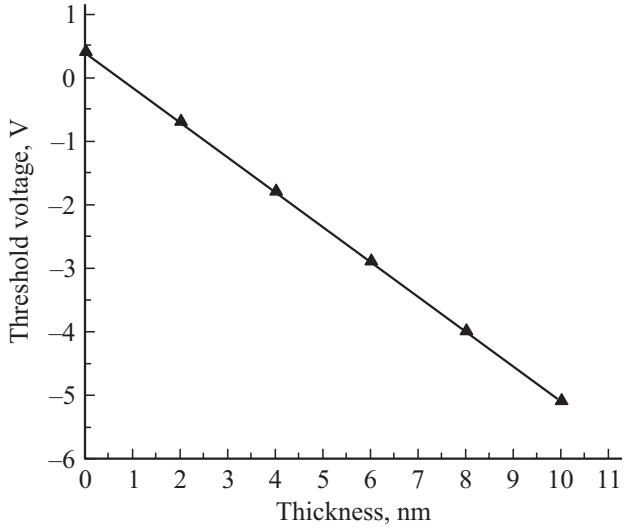

Figure 4. Plot of threshold voltage with the variation of barrier thickness at constant oxide thickness of 6 nm.

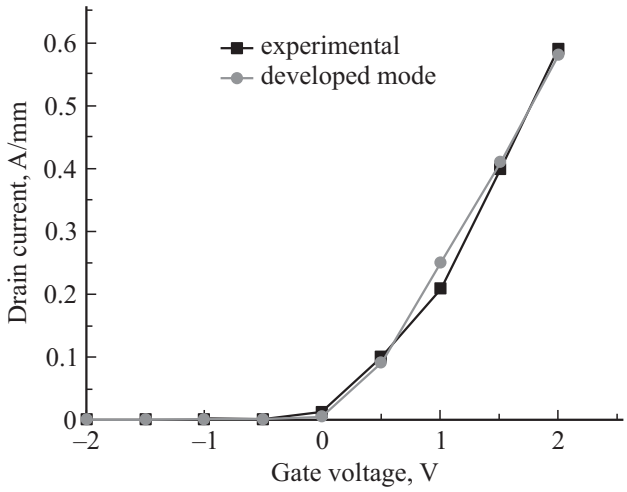

Figure 5. Plot of drain current with respect to gate voltage at $V_{ds} = 5$ V with experimental results from Ref. [8].

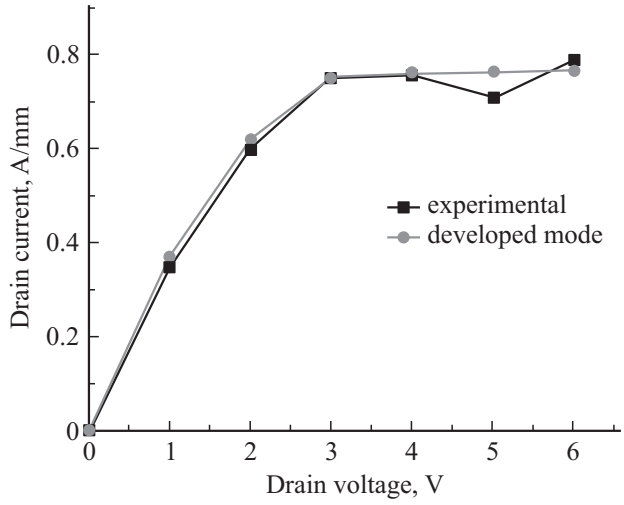

Figure 6. Plot of drain current with respect to drain voltage at $V_{gs} = 2.5$ V with experimental results from Ref. [8].

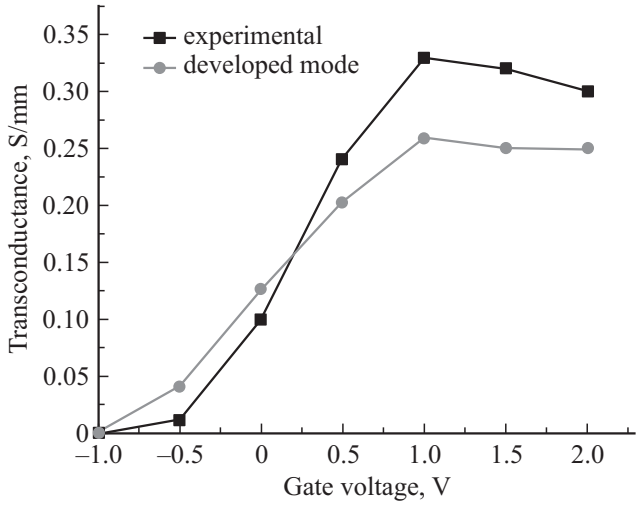

Figure 7. Plot of transconductance with respect to gate voltage with experimental results from Ref. [8].

maintain the shape. Then the characteristics obtained from the developed models are compared with the experimental results obtained in Ref. [8] and are shown in Figs 5 and 6. Similarly the variation of transconductance with V_{gs} is shown in Fig. 7. The parameters of the AlN/GaN heterostructure used for solving the model equations in MATLAB are also taken from existing literatures and indicated as follows.

From the above plots we can observe that the characteristics obtained from solving the model equations are in good agreement with the experimental results. In Fig. 5 we obtained a threshold voltage of 0.1 V for $V_{ds} = 5$ V and gate length $L_g = 210$ nm. Similarly in Fig. 6 the saturation drain current of 760 mA/mm is obtained with $V_{gs} = 2.5$ V which is similar to that of experimental results. The peak transconductance of 0.26 S/mm is obtained from the developed model as shown in Fig. 7, which is approximately equal to the transconductance of 0.33 S/mm obtained as per the experimental data [8].

4. Conclusion

In this paper the authors have attempted to establish an analytical model for predicting current–voltage and transconductance characteristics of the proposed normally-off AlN/GaN MOSHEMT by developing suitable models for threshold voltage and quantum capacitance in the 2DEG, which is formed at the heterointerface of AlN/GaN. It is also observed here that a positive threshold voltage is obtained by decreasing the barrier thickness which leads to a normally-off MOSHEMT. The predicted $I_d - V_{gs}$, $I_d - V_{ds}$ and transconductance characteristics are in good agreement with the experimental results available from the literature and hence validate the developed model.

References

[1] A.M. Dabiran, A.M. Wowchak, A. Osinsky, J. Xie, B. Hertog, B. Cui, D.C. Look, P.P. Chow. Appl. Phys. Lett., **93**, 82 111 (2008).
[2] T.R. Lenka, A.K. Panda. Semiconductors, **45** (9), 1211 (2011).
[3] T.R. Lenka, A.K. Panda. Semiconductors, **45** (5), 660 (2011).
[4] M. Miyoshi, M. Sakai, S. Arulkumaran, H. Ishikawa, T. Egawa, M. Tanaka, O. Oda. Jpn. J. Appl. Phys., **43** (12), 7939 (2004).
[5] S. Hubbard, D. Pavlidis, V. Valiaev, A. Eisenbach. J. Electron. Mater., **31**, 395 (2002).
[6] P. Ye, B. Yang, K. Ng, J. Bude, G. Wilk, S. Halder, J. Hwang. Inter. J. High Speed Electronics and Systems, **14** (3), 791 (2004).
[7] T. Huang, X. Zhu, K.M. Lau. IEEE Electron Devices Lett., **33** (8), 1123 (2012).
[8] T. Huang, X. Zhu, K.M. Lau. IEEE Trans. Electron Devices, **60** (10), 3019 (2013).
[9] S. Khandelwal, T.A. Fjeldly. Solid State Electron., **76**, 60 (2012).
[10] F.M. Yigletu, S. Khandelwal. IEEE Trans. Electron Devices, **60** (11), 3746 (2013).
[11] D. Pandey, T.R. Lenka. Semiconductors, **49** (4), 524 (2015).
[12] O. Ambacher, J. Smart, J.R. Shealy, N.G. Weimann, K. Chu, M. Murphy, W.J. Schaff, L.F. Eastman. J. Appl. Phys., **85** (6), 3222 (1999).
[13] S. Ganguly, J. Verma, G. Li, T. Zimmermann, H. Xing, D. Jena. Appl. Phys. Lett., **99**, 193 504 (2011).
[14] M. Tapajna, J. Kuzmík. Appl. Phys. Lett., **100**, 1135 091 (2012).
[15] S. Kola, J.M. Golio, G.N. Maracas. IEEE Electron Device Lett., **9** (3), 136 (1988).
[16] M. Li, Y. Wang. IEEE Trans. Electron Devices, **55** (1), 261 (2008).
[17] X. Cheng, M. Li, Y. Wang. IEEE Trans. Electron Devices, **56** (12), 2881 (2009).
[18] Y.Q. Tao, D.J. Chen, Y.C. Kong, B. Shen, Z.L. Xie, P. Han, R. Zhang, Y.D. Zheng. J. Electron. Mater., **35** (4), 722 (2006).
[19] D.A. Deen, J.G. Champlain. Appl. Phys. Lett., **99**, 53501 (2011).
[20] S.M. Sze. *Physics of Semiconductor Devices,* 3rd edn. (John Wiley & Sons, 2007).

Редактор Л.В. Шаронова